Parameter extraction of solar photovoltaic models using an improved whale optimization algorithm

Guojiang Xiong[a,*], Jing Zhang[a], Dongyuan Shi[b], Yu He[a]

[a] Guizhou Key Laboratory of Intelligent Technology in Power System, College of Electrical Engineering, Guizhou University, Guiyang 550025, China
[b] State Key Laboratory of Advanced Electromagnetic Engineering and Technology, Huazhong University of Science and Technology, Wuhan 430074, China

ABSTRACT

Parameter extraction of solar photovoltaic (PV) models is a typical complex nonlinear multivariable strongly coupled optimization problem. In this paper, an improved whale optimization algorithm (WOA), referred to as IWOA, is proposed to accurately extract the parameters of different PV models. The original WOA has good local exploitation ability, but it is likely to stagnate and suffer from premature convergence when dealing with complex multimodal problems. To conquer this concerning shortcoming, IWOA develops two prey searching strategies to effectively balance the local exploitation and global exploration, and thereby enhance the performance of WOA. Three benchmark test PV models including single diode, double diode and PV module models, and two practical PV power station models with more modules in the Guizhou Power Grid of China are employed to verify the performance of IWOA. The experimental and comparison results comprehensively demonstrate that IWOA is significantly better than the original WOA and three advanced variants of WOA, and is also highly competitive with the reported results of some recently-developed parameter extraction methods.

1. Introduction

Solar energy has gained the highest attention (highest growth rate) worldwide in the last years due to its potential availability, good visibility, and safe use for small and large scales by residential, commercial, and utility-scale users [1]. China, for example, added about 42 GW of solar photovoltaic (PV) power capacity in the first nine months of 2017, and the total PV installed capacity has risen to 119 GW [2]. In such a context, the PV system, which directly converts solar energy into electricity, has attracted increasing attention in recent years. In order to study the dynamic conversion behavior of a PV system, one first needs to know how to model its basic device, i.e., the PV cell. Many approaches have been developed to model PV cells and the most popular one is the use of equivalent circuit models [3]. Among which the widely used circuit models are the single diode model and double diode model. After selecting an appropriate model structure, the accuracy of the parameters associated with the structure is crucial for modeling, sizing, performance evaluation, control, efficiency computations and maximum power point tracking of solar PV systems [4,5]. However, these model parameters, in general, are unavailable and changeable due to the following two reasons. On one hand, the manufacturers usually provide only the open circuit voltage, short circuit current, maximum

power point current, and voltage under standard test condition (STC). But the actual environmental conditions are always changing and are far from the STC. On the other hand, the value of these parameters changes over time due to the PV degradation [6]. Therefore, how to achieve or extract accurate parameters is of high importance and significance, and has been highly attracted by researchers [4].

In order to handle this complex yet important problem, a good number of methods have been proposed. These methods can be divided into two types: analytical methods [7–15] and optimization methods. The former, mainly based on the key data points provided by the manufacturers, utilizes mathematical equations to derive the model parameters. However, we know that the value of these points is achieved under the STC and thereby they are not enough to predict accurate current–voltage (*I-V*) characteristic curves under varying insolation and temperature levels [16]. With regard to the optimization methods, they can be further categorized into deterministic and heuristic methods from the algorithmic perspective. Both methods transform the parameter extraction problem into an optimization problem and then use some reference points of a given *I-V* characteristic curve to extract the parameters. The deterministic methods, including the least squares (Newton-based method) [17], Lambert W-functions [18], iterative curve fitting [19], impose various restrictions such as

Nomenclature

a	parameter linearly decreased from 2 to 0
A, C	coefficients
b	constant
D	dimension of individual vector
I_d	diode current (A)
I_L	output current (A)
I_{ph}	photo generated current (A)
I_{sd}, I_{sd1}, I_{sd2}	saturation currents (A)
I_{sh}	shunt resistor current (A)
k	Boltzmann constant ($1.3806503 \times 10^{-23}$ J/K)
l, p	random real numbers in (0, 1)
n, n_1, n_2	diode ideality factors
N	number of experimental data
N_p	number of cells connected in parallel
N_s	number of cells connected in series
ps	size of population
q	electron charge ($1.60217646 \times 10^{-19}$ C)
R_s	series resistance (Ω)
R_{sh}	shunt resistance (Ω)
t	current iteration
T	cell temperature (K)
VL	output voltage (V)
Vt	diode thermal voltage (V)
x	extracted parameters vector
$x_{i,d}$	dth parameter of ith individual vector
Xi	ith individual vector
Xg	best position found so far
X_r, X_{r1}, X_{r2}	random individual vectors
I-V	current–voltage
P-V	power–voltage
PV	photovoltaic
RMSE	root mean square error
Min	minimum RMSE
Max	maximum RMSE
Mean	mean RMSE
Std Dev	standard deviation
WOA	whale optimization algorithm
CWOA	chaotic WOA
IWOA	improved WOA
LWOA	Lévy flight trajectory-based WOA
PSO-WOA	hybrid particle swarm optimization-WOA
STC	standard test condition

continuity, convexity, and differentiability on the objective functions. In addition, they are sensitive to the initial condition and gradient information and thereby are easily trapped into local optima when dealing with complex multimodal problems. These limitations make the deterministic methods encounter many difficulties and challenges when solving the nonlinear multimodal parameter extraction problem. Alternatively, the heuristic methods have no strict requirements on the form of optimization problems and can avoid the influences of the initial condition sensitivity and gradient information. Consequently, they have received considerable attention recently. The successfully implemented heuristic methods for the parameter extraction of PV models include genetic algorithm (GA) [20,21], particle swarm optimization (PSO) [22–24], differential evolution (DE) [25–28], artificial bee colony (ABC) [29], biogeography-based optimization (BBO) [30], harmony search (HS) [31], bacterial foraging algorithm (BFA) [32,33], teaching–learning-based optimization (TLBO) [34–36], water cycle algorithm (WCA) [37,38], flower pollination algorithm (FPA) [39], bird mating optimizer (BMO) [40], multi-verse optimizer (MVO) [41], asexual reproduction optimization (ARO) [42], fireworks algorithm (FWA) [43], cat swarm optimization (CSO) [44], ant lion optimizer (ALO) [45], moth-flame optimization (MFO) [46], hybrid methods [47–52], etc.

Whale optimization algorithm (WOA), proposed in 2016 [53], is a very young yet powerful population-based heuristic method inspired by the special spiral bubble-net hunting behavior of humpback whales. It has already proven a worthy optimization method compared with other popular population-based methods such as GA, PSO, and DE. Owing to its simplicity and efficiency, WOA has been successfully applied to various fields, such as reactive power dispatch [54], neural network [55], image segmentation [56], and feature selection [57], wind speed forecasting [58].

However, similar to other population-based methods, WOA also faces up to some challenges. One typical issue in point is that, it converges fast in the very beginning of the evolutionary process, but it is easily trapped into local search later and thereby suffers from prematurity when solving multimodal problems. The main reason is that, for a population-based method, it is well known that both the global exploration and local exploitation are indispensable. However, they are usually in conflict in practice. In such a context, it is important to balance them, especially in dealing with complex multimodal problems. With regard to the original WOA, it is good at exploiting the local

search space, but lacks enough global exploration ability to jump out of local optima. In order to remedy the drawback mentioned, an improved WOA variant, referred to as IWOA, is proposed in this paper. IWOA, which develops two prey searching strategies to enhance the performance of WOA, is able to effectively balance the local exploitation and global exploration. The experimental and comparison results comprehensively demonstrate that IWOA is able to conquer premature convergence and to accelerate the global searching process simultaneously.

The main contributions of this work are as follows:

(1) An improved WOA method, IWOA, is proposed for the parameter extraction of PV models. IWOA, based on the deep analysis of the drawback of the original WOA, employs two proposed prey searching strategies to effectively balance the exploitation and exploration.

(2) IWOA is applied to three benchmark test PV models and two practical PV power station models with more modules in the Guizhou Power Grid of China. Multiple performance aspects including solution quality, convergence speed, robustness, and statistics are evaluated to comprehensively verify the effectiveness of IWOA.

(3) The performance of IWOA is extensively compared with the original WOA and three advanced variants of WOA, as well as those reported results of some recently-proposed parameter extraction methods. The comparison results consistently demonstrate that IWOA is highly competitive and can be used as an effective alternative to solve the parameter extraction problem of PV models.

The remainder of this paper is organized as follows. Section 2 presents the original WOA and the proposed IWOA. Section 3 briefly introduces the PV models and the mathematical formulation of parameter extraction problem. In Section 4, experimental results and comparisons are provided. Finally, Section 5 is devoted to conclusions and future work.

2. Improved whale optimization algorithm

2.1. Whale optimization algorithm (WOA)

WOA [53] is a very young yet powerful population-based algorithm inspired by the special spiral bubble-net hunting behavior of humpback

whales. In WOA, each population individual is denoted as $X_i = [x_{i,1}, x_{i,2}, ..., x_{i,D}]$, where $i = 1, 2, ..., ps$, ps is the population size and D is the problem dimension. WOA consists of three searching steps: encircling prey, bubble-net attacking method, and searching for prey.

2.1.1. Encircling prey

WOA assumes that the current best candidate solution is the target prey which is defined as the best search agent. After determining the best search agent, other humpback whales will attempt to update their positions towards the agent. This behavior can be formulated as follows [53]:

$$S = |C \cdot X_g - X^t| \tag{1}$$

$$X^{t+1} = X_g - A \cdot S \tag{2}$$

where t denotes the current iteration. $|\cdot|$ denotes the absolute value. X_g denotes the best position found so far. A and C are coefficients and are respectively calculated as follows:

$$A = 2 \cdot a \cdot rand(0, 1) - a \tag{3}$$

$$C = 2 \cdot rand(0, 1) \tag{4}$$

where a is linearly decreased from 2 to 0 over the course of iterations. $rand(0,1)$ is a uniformly distributed random real number in $(0,1)$.

2.1.2. Bubble-net attacking method

In the process of bubble-net attacking, humpback whales simultaneously utilize two strategies, i.e., shrinking encircling and spiraling to spin around the prey to update their positions. WOA assumes that both strategies have the same probability to be performed. These two strategies are mathematically expressed as follows, respectively [53]:

$$X^{t+1} = X_g - A \cdot S \text{ if } p < 0.5 \tag{5}$$

$$X^{t+1} = S' \cdot \exp(bl) \cdot \cos(2\pi l) + X_g \text{ if } p \geqslant 0.5 \tag{6}$$

where $S' = |X_g - X^t|$. b is a constant for defining the shape of the logarithmic spiral. l and p are random real numbers in $(0,1)$.

2.1.3. Searching for prey

In practice, humpback whales swim randomly to search for prey. Their positions are updated according to the information of each other. The coefficient A can be used to determine whether to force a whale to move far away from a reference whale. A whale will update its position by using a random whale instead of the best one if $|A| \geqslant 1$ hold, This mathematical model can be formulated as follows [53]:

$$S = |C \cdot X_r^t - X^t| \tag{7}$$

$$X^{t+1} = X_r^t - A \cdot S \tag{8}$$

where r is a random whale.

The flowchart of WOA is shown in Fig. 1 and the corresponding main procedure is given in Appendix A.

2.2. Improved whale optimization algorithm (IWOA)

The original WOA has already proven itself a worthy optimization method. However, similar to other population-based algorithms, WOA also faces up to some challenges. It converges fast in the very beginning of the evolutionary process, but it is easily trapped into local search later and thereby suffers from prematurity when solving multimodal problems. The concrete reason is that, WOA utilizes the coefficient A to balance the exploration and exploitation in two ways. On one hand, Eqs. (8) and (2) are selectively performed to reinforce the exploration and exploitation, respectively. However, the probabilities of performing these two Equations are not equal or balanced due to the following reason.
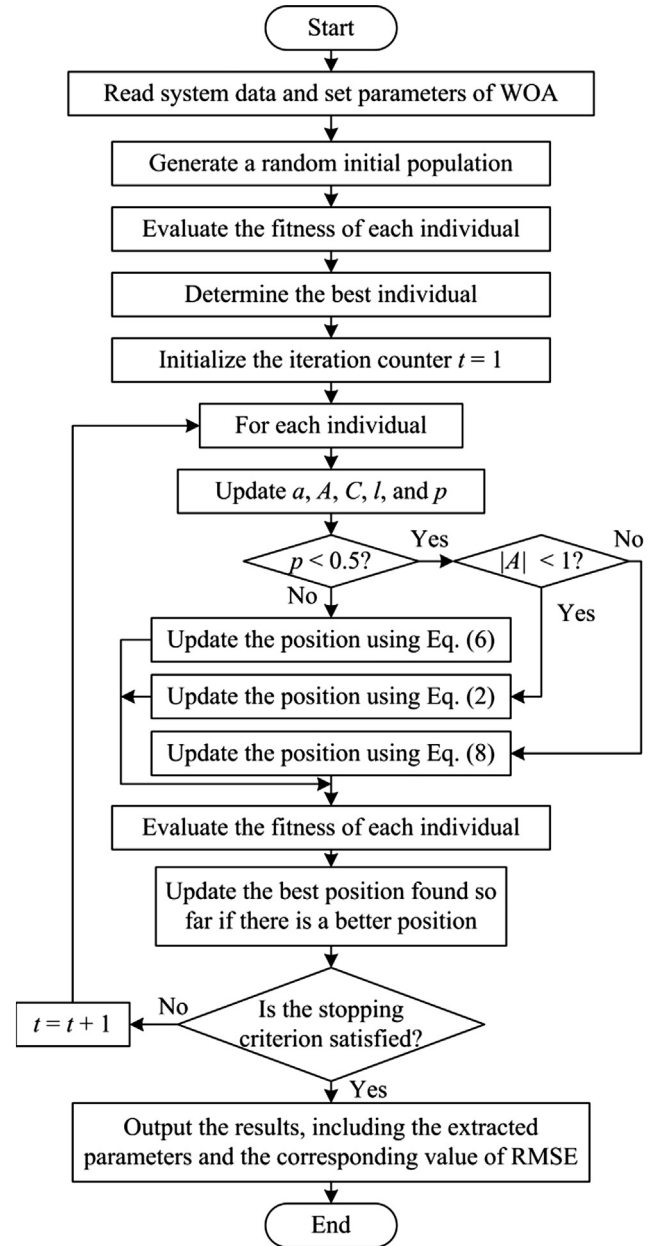
Eq. (3) can be rewritten as:

Fig. 1. The flowchart of WOA.

$$A = 2 \cdot a \cdot rand(0, 1) - a$$
$$= [2 \cdot rand(0, 1) - 1] \cdot a$$
$$= \lambda \cdot a \tag{9}$$

where $\lambda = 2 \cdot rand(0, 1) - 1$ is a uniformly distributed random real number in $(-1,1)$. Because a is linearly decreased from 2 to 0 over the course of iterations, therefore $|A| = |\lambda \cdot a| < 1$ always hold in the second half of the evolutionary process in which Eq. (2) is always performed consequently. In the first half of the evolutionary process, the probability of performing Eq. (2) can be calculated as follows:

$$P(|A| < 1) = P(|\lambda \cdot a| < 1) = 0.5 + \int_{0.5}^{1} \int_{1}^{1/\lambda} da d\lambda$$
$$= 0.5 + \int_{0.5}^{1} \left(\frac{1}{\lambda} - 1\right) d\lambda = 0.5 + (\ln \lambda - \lambda) \Big|_{0.5}^{1}$$
$$= \ln 2 \approx 0.693 \tag{10}$$

It can be seen that even if in the first half of the evolutionary process, Eq. (2) has a larger probability of being selected. In fact, the total probability of performing Eq. (2) throughout the whole evolutionary

process is $P(|A| < 1) = 0.5 + 0.5 \times \ln 2 \approx 0.847$ under the precondition $p < 0.5$. Therefore, Eq. (2) highly dominates Eq. (8).

On the other hand, in the early evolutionary process, A is relatively big and can provide a large perturbation to help WOA jump out of local optima. But it is quickly decreased with the progress of evolution and thus the perturbation is too small to be beneficial for the exploration.

From the above analysis, we know that WOA overemphasizes the exploitation, which easily leads to the prematurely converging to local optima. In order to remedy the defect of the original WOA and balance the exploitation and exploration effectively, in this paper, an improved WOA, referred to as IWOA, is proposed. In IWOA, the following two prey searching strategies, i.e., Eqs. (11) and (12) are developed to replace Eqs. (8) and (2), respectively.

$$X_i^{t+1} = X_{r1}^t - A \cdot |X_i^t - X_{r1}^t| \tag{11}$$

$$X_i^{t+1} = X_{r2}^t - A \cdot |X_g - X_{r2}^t| \tag{12}$$

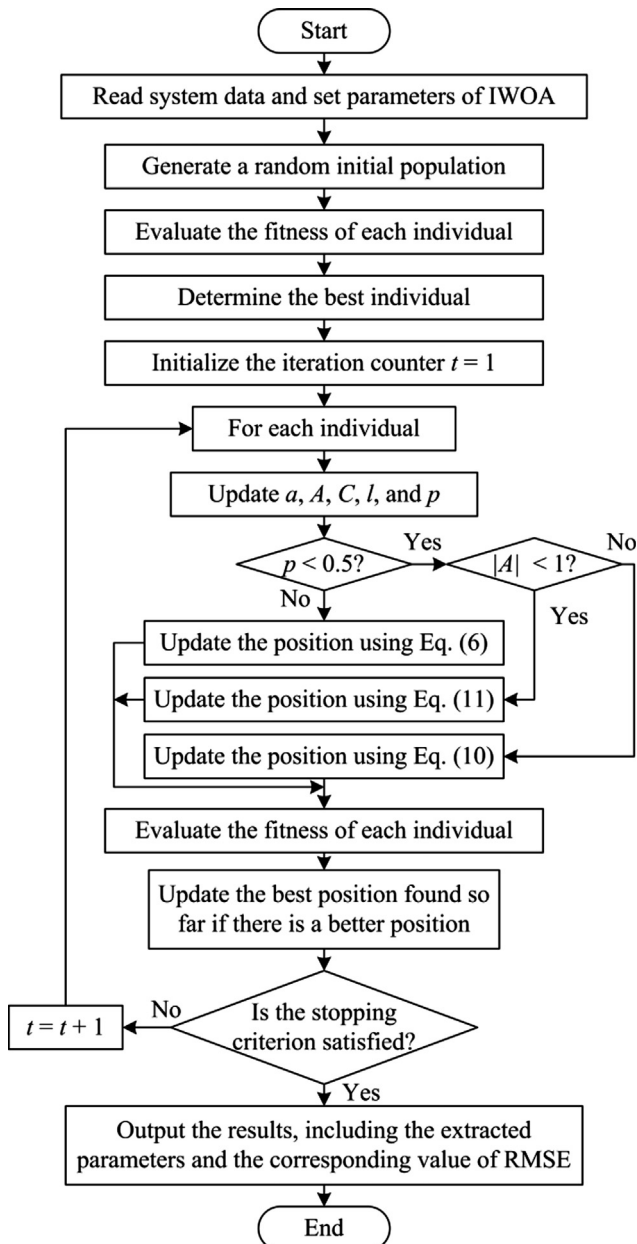where $r1$ and $r2$ are two random individuals. The core idea of the proposed searching strategies is based on three considerations. First, Eq. (12) utilizes X_{r2}^t instead of X_g as the base and employs $A \cdot |X_g - X_{r2}^t|$ to offer a symmetrical perturbation on X_{r2}^t, which is able to increase the population diversity. Second, although Eq. (12) still dominates Eq. (11), both Equations employ random individuals to update the current individual, which is able to enhance the exploration on the basis of the existing exploitation and therefore to achieve a good equilibrium between them. Third, the abandonment of the coefficient C can guarantee the consistency of the distance between two individuals and thereby facilitate the robustness. The flowchart of IWOA is presented in Fig. 2 and the corresponding main procedure is given in Appendix B. It is worth noting that IWOA keeps the basic structure of the original WOA and it does not introduce additional parameter that needs to be tuned or other complex searching operators. Therefore, the time complexity of both algorithms is the same and equals to $O(t_{\max} \cdot ps \cdot D)$, where $t_{\max}$ is the maximum number of iteration.

To show the effectiveness and efficiency of IWOA, a two-dimensional Schwefel function $f(X) = D \times 418.9829 + \sum_{i=1}^{D} -x_i \sin(\sqrt{|x_i|})$ [59] is taken for example. The minimum value of this function is 0 at its global solution (420.9867, 420.9867, …,420.9867). The search range is $[-500, 500]^D$. Schwefel function, as shown in Fig. 3, is a complex multimodal function whose surface is composed of a great number of peaks and valleys. It has a second best minimum far from the global minimum where many algorithms are trapped. Furthermore, the global minimum is near the bounds of the domain. Therefore, the function places high demand for the optimization algorithms. Note that both WOA and IWOA are executed from the same initial random population, so any difference of their performance is attributed to their prey searching strategies. The distributions of population at different evolutionary processes and the convergence curves are potted in Fig. 4. It is shown that the population distributions of WOA are almost unchanged from the 50th iteration to the 100th iteration, meaning that WOA has been trapped into local optimum and suffered from prematurity. Quite the opposite, the individuals of IWOA can swarm quickly together towards the global minimum. Moreover, the convergence characteristics further validate the above declaration from another perspective. As stated previously, WOA converges very fast in the very beginning of the evolutionary process, but it is inclined to appear premature convergence and stagnation behavior. The phenomenon fully demonstrates that WOA has good local exploitation ability but lacks effective global exploration ability. With regard to IWOA, it is able to maintain a rapid convergence speed throughout the whole evolutionary process and finally to achieve the global minimum, which means that IWOA can yield

Fig. 2. The flowchart of IWOA.
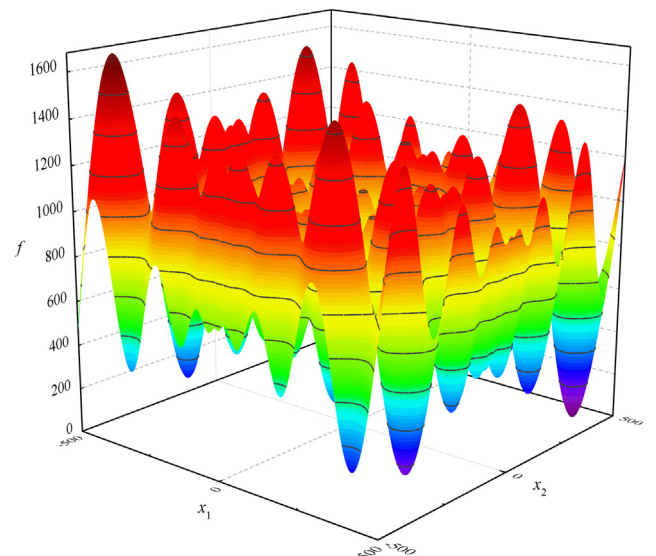
Fig. 3. Schwefel function.
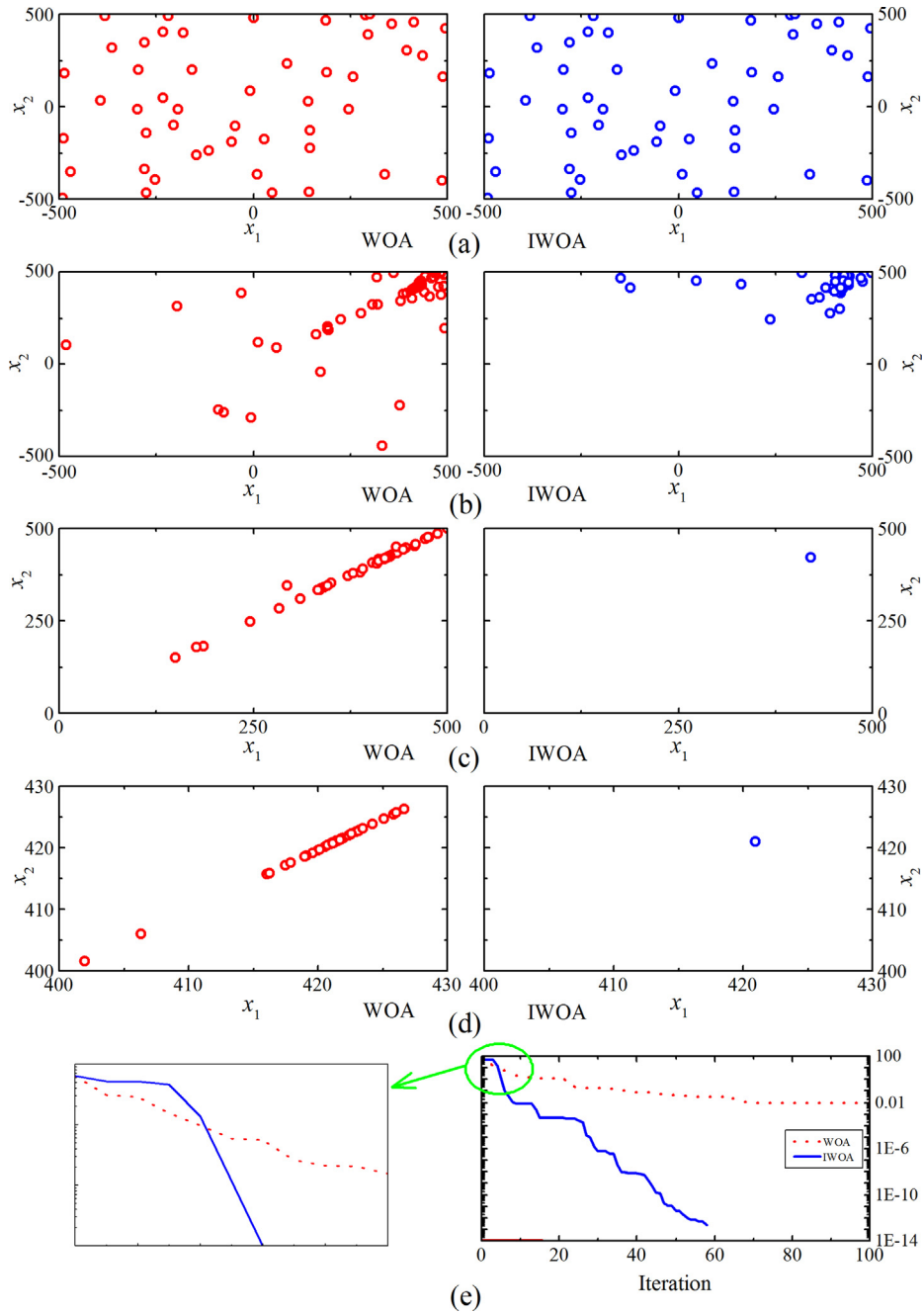
Fig. 4. Population distributions of WOA and IWOA observed at different stages and both algorithms' convergence characteristics associated with the example of a two-dimensional Schwefel function. (a) Initial population distribution. (b) Population distribution at iteration = 10. (c) Population distribution at iteration = 50. (d) Population distribution at iteration = 100. (e) Convergence curves.

a strong balance between the exploitation and exploration.

3. Problem formulation

Many PV models have been developed to describe the *I-V* characteristics of PV cells. Among them, the widely used models are the single diode and double diode models.

3.1. Single diode model

The equivalent circuit of single diode model is shown in Fig. 5. The output current I_L can be calculated as follows [3,4,29,31,60,61]:

$$I_L = I_{ph} - I_d - I_{sh} \tag{13}$$
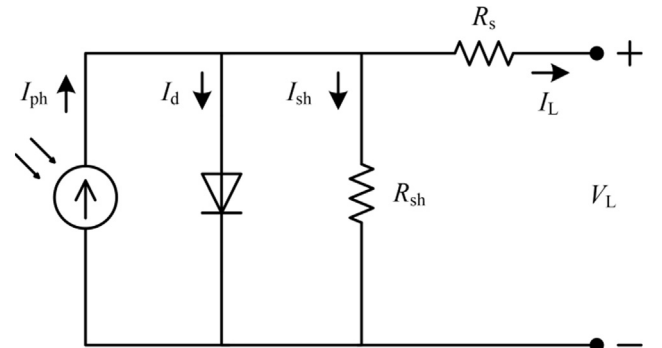
Fig. 5. Equivalent circuit of the single diode model.

where I_{ph} denotes the photo generated current. I_d denotes the diode current. I_{sh} denotes the shunt resistor current.

According to the Shockley equation, I_d can be calculated as follows [3,4]:

$$I_d = I_{sd} \cdot \left[\exp\left(\frac{V_L + R_s \cdot I_L}{nV_t} \right) - 1 \right] \tag{14}$$

where I_{sd} denotes the saturation current. V_L denotes the output voltage. R_s denotes the series resistance. n denotes the diode ideal factor. V_t denotes the thermal voltage of the diode and is calculated as follows [6]:

$$V_t = \frac{kT}{q} \tag{15}$$

where k is the Boltzmann constant ($1.3806503 \times 10^{-23}$ J/K). q is the electron charge ($1.60217646 \times 10^{-19}$ C). T is the cell temperature (K).

I_{sh} can be calculated as follows [26]:

$$I_{sh} = \frac{V_L + R_s \cdot I_L}{R_{sh}} \tag{16}$$

where R_{sh} denotes the shunt resistance.

Hence, Eq. (13) can be rewritten as follows:

$$I_L = I_{ph} - I_{sd} \cdot \left[\exp\left(\frac{V_L + R_s \cdot I_L}{nV_t} \right) - 1 \right] - \frac{V_L + R_s \cdot I_L}{R_{sh}} \tag{17}$$

It is known from Eq. (17) that there are five unknown parameters (i.e., I_{ph}, I_{sd}, R_s, R_{sh}, and n) that need to be extracted.

3.2. Double diode model

The single diode model is highly preferred, especially for c-Si based solar cells, due to its accuracy and simplicity [3]. It is mathematically valid for almost all types but there are some physical problems when it is applied to thin films. It can behave satisfactorily under normal operating conditions but the performance is frequently far from ideal at low irradiance. In practice, the current source is also shunted by another diode that models the space charge recombination current and a shunt leakage resistor to account for the partial short circuit current path near the cell's edges due to the semiconductor impurities and non-idealities [29,31]. In this context, the double diode model, as shown in Fig. 6, is developed to take the effect of recombination current loss in the depletion region into account. Although it is relatively complex, it can exhibit superior behavior at low irradiance and thus is attractive. The output current can be calculated as follows [3,4,61–63]:

$$\begin{aligned} I_L &= I_{ph} - I_{d1} - I_{d2} - I_{sh} \\ &= I_{ph} - I_{sd1} \cdot \left[\exp\left(\frac{V_L + R_s \cdot I_L}{n_1 V_t} \right) - 1 \right] \\ &\quad - I_{sd2} \cdot \left[\exp\left(\frac{V_L + R_s \cdot I_L}{n_2 V_t} \right) - 1 \right] - \frac{V_L + R_s \cdot I_L}{R_{sh}} \end{aligned} \tag{18}$$
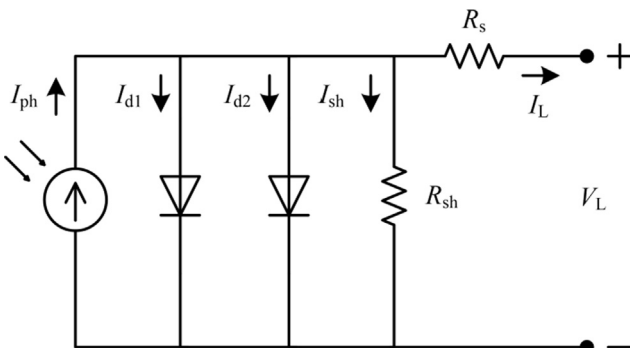

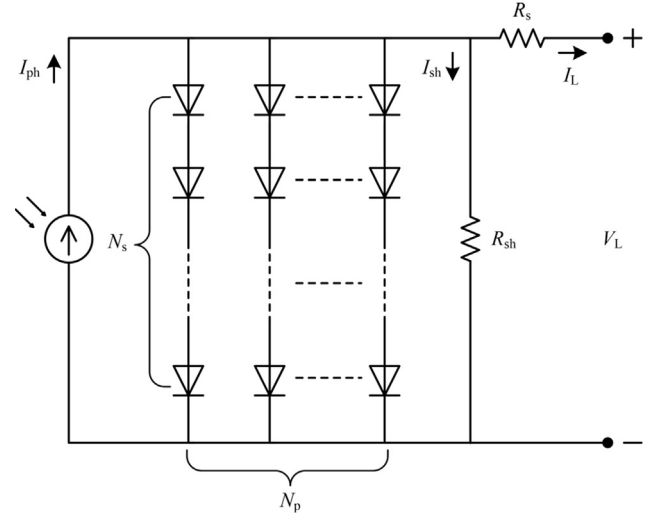**Fig. 6.** Equivalent circuit of the double diode model.

Fig. 7. Equivalent circuit of the PV module model.

where I_{sd1} and I_{sd2} denote the diffusion and saturation currents, respectively. n_1 and n_2 denote the diffusion and recombination diode ideal factors, respectively. In this PV model, there are seven unknown parameters (i.e., I_{ph}, I_{sd1}, I_{sd2}, R_s, R_{sh}, n_1 and n_2) that need to be extracted.

3.3. PV module model

A typical single diode based PV module model which consists of $N_s \times N_p$ solar cells in series and/or in parallel is illustrated in Fig. 7. The output current can be formulated as follows [33,64,65]:

$$I_L = N_p \left\{ I_{ph} - I_{sd} \cdot \left[\exp\left(\frac{V_L/N_s + R_s I_L/N_p}{nV_t} \right) - 1 \right] - \frac{V_L/N_s + R_s I_L/N_p}{R_{sh}} \right\} \tag{19}$$

As with the single diode model, this model also has five unknown parameters (i.e., I_{ph}, I_{sd}, R_s, R_{sh}, and n) that need to be extracted.

3.4. Objective function

Extraction of the unknown parameters for PV models can be easily transformed into an optimization problem. The goal of the resultant optimization problem is to minimize the error between the experimental data and the calculated data based on the *I-V* characteristic. Generally, the root mean square error (RMSE) between the measured current and the calculated current is used as the objective function:

$$\min F(\boldsymbol{x}) = \text{RMSE}(\boldsymbol{x}) = \sqrt{\frac{1}{N} \sum_{k=1}^{N} f_k(V_L, I_L, x)^2} \tag{20}$$

where N is the number of experimental data. $\boldsymbol{x}$ is the set of the extracted parameters.

For the single diode model, $f_k(V_L, I_L, x)$ and x are respectively as follows:

$$f_k(V_L, I_L, x) = I_{ph} - I_{sd} \cdot \left[\exp\left(\frac{V_L + R_s \cdot I_L}{nV_t} \right) - 1 \right] - \frac{V_L + R_s \cdot I_L}{R_{sh}} - I_L \tag{21}$$

$$x = \backslash \{ I_{ph}, I_{sd}, R_s, R_{sh}, n \backslash \} \tag{22}$$

For the double diode model, $f_k(V_L, I_L, x)$ and x are respectively as follows:

$$f_k(V_L, I_L, x) = I_{ph} - I_{sd1} \cdot \left[\exp\left(\frac{V_L + R_s \cdot I_L}{n_1 V_t}\right) - 1 \right]$$
$$- I_{sd2} \cdot \left[\exp\left(\frac{V_L + R_s \cdot I_L}{n_2 V_t}\right) - 1 \right]$$
$$- \frac{V_L + R_s \cdot I_L}{R_{sh}} - I_L \tag{23}$$

$$x = \backslash\{ I_{ph}, I_{sd1}, I_{sd2}, R_s, R_{sh}, n_1, n_2 \backslash\} \tag{24}$$

For the PV module model, $f_k(V_L, I_L, x)$ and x are respectively as follows:

$$f_k(V_L, I_L, x) = N_p \left\{ I_{ph} - I_{sd} \cdot \left[\exp\left(\frac{V_L / N_s + R_s I_L / N_p}{n V_t}\right) - 1 \right] \atop - \frac{V_L / N_s + R_s I_L / N_p}{R_{sh}} \right\} - I_L \tag{25}$$

$$x = \backslash\{ I_{ph}, I_{sd}, R_s, R_{sh}, n \backslash\} \tag{26}$$

4. Case studies

4.1. Experimental settings

For the following experiments, the population size ps and the maximum number of iteration are set to be 50 and 2000, respectively. In addition, the original WOA and three advanced variants of WOA, i.e., CWOA [67], LWOA [68], and PSO-WOA [69] are employed for comparison. The involved methods use the same parameters as those in their original literature except the population size ps which is set to be 50 for fair comparison. A number of 50 independent runs are conducted to eliminate contingency. All experiments are executed on a 3.7-GHz Intel(R) Core(TM) computer with 8.0-GB RAM under MATLAB 2010b.

4.2. Experimental results on benchmark test PV models

To validate the performance of IWOA on the parameter extraction problem of PV models, IWOA is firstly applied to three benchmark test PV models including single diode, double diode, and single diode based PV module models. Their experimental I-V data are acquired from [66], where a 57 mm diameter commercial silicon solar cell (R.T.C. France) operating under 1000 W/m² at 33 °C and a solar module (Photowatt-PWP201) which consists of 36 polycrystalline silicon cells in series operating under 1000 W/m² at 45 °C. The search ranges of the involved parameters for these three benchmark test PV models are tabulated in Table 1.

4.2.1. Solution quality

The experimental results including the minimum (Min), maximum (Max), mean RMSE and standard deviation (Std Dev) values of the single diode, double diode, and PV module models are summarized in Tables 2–4, respectively. Some recently-developed methods' reported results are also listed in these Tables for comparison. It can be seen from Tables 2–4 that the proposed IWOA significantly outperforms WOA, CWOA, LWOA, and PSO-WOA on all three PV models in terms of minimum, maximum, and mean RMSE values. When compared with those recently-developed methods, IWOA is also highly competitive.

Table 1
Search range of parameters for the benchmark test PV models.

Parameter	Single/double diode model		PV module model	
	Lower bound	Upper bound	Lower bound	Upper bound
I_{ph} (A)	0	1	0	2
I_{sd} (µA)	0	1	0	50
R_s (Ω)	0	0.5	0	2
R_{sh} (Ω)	0	100	0	2000
n, n_1, n_2	1	2	1	50

Table 2
Comparison of experimental results for the single diode model.

Method	Min	Max	Mean	Std. dev.
Rcr-IJADE [26]	9.860219E−04	9.860219E−04	9.860219E−04	5.12E−16
ABSO [29]	9.9124E−04	NA	NA	NA
BBO-M [30]	9.8634E−04	NA	NA	NA
GGHS [31]	9.9078E−04	NA	NA	NA
SATLBO [34]	9.86022E−04	9.94939E−04	9.87795E−04	2.30015E−06
GOTLBO [35]	9.87442E−04	1.98244E−03	1.33488E−03	2.99407E−04
BMO [40]	9.8608E−04	NA	NA	NA
CARO [42]	9.8665E−04	NA	NA	NA
IJAYA [64]	9.8603E−04	1.0622E−03	9.9204E−04	1.4033E−05
PS [70]	2.863E−01	NA	NA	NA
SA [71]	1.70E−03	NA	NA	NA
MSSO [72]	9.8607E−04	NA	NA	NA
CWOA [73]	9.8604E−04	NA	NA	1.0216E−08
WOA	1.0480E−03	9.1992E−03	3.0808E−03	2.2147E−03
CWOA	1.1812E−03	4.5404E−02	7.3931E−03	9.4349E−03
LWOA	1.2352E−03	1.1514E−02	3.3372E−03	2.4418E−03
PSO-WOA	1.1983E−03	3.1442E−03	1.9991E−03	4.7346E−04
IWOA	9.8602E−04	1.0331E−03	9.9524E−04	1.1267E−05

NA: Not available in the literature.

For the single diode model, IWOA, Rcr-IJADE, and SATLBO achieve the least RMSE value (9.8602E−04) which is better than that of other methods. For the double diode model, although IWOA yields the second best RMSE value (9.8255E−04) which is slightly bigger than that (9.8248E−04) of Rcr-IJADE, the difference is very small. For the PV module model, IWOA, Rcr-IJADE, SATLBO, and IJAYA can obtain the best RMSE value (2.4251E−03).

Corresponding to the best RMSE value of each method, the values of parameters for single diode, double diode, and PV module models are listed in Tables 5–7, respectively. The results also include the reported results of some recently-developed methods. It can be seen that the values of the parameters extracted by different methods are very close to each other. Based on the extracted parameters, the current corresponding to the measured voltage is calculated and summarized in Tables 8–10, respectively. In addition, for ease of comparison, the sum of individual absolute error (SIAE) defined as follows is employed:

$$\text{SIAE} = \sum_{item}^{N} |I_{item,measured} - I_{item,calculated}| \tag{27}$$

The SIAE of each involved method is listed in Tables 8–10 for the three benchmark test PV models, respectively. From the results, it is clear to observe that the current data generated by IWOA are highly coinciding with the measured data. The SIAE value of IWOA is smaller than that of the original WOA about 3.81%, 10.88%, and 0.67%, respectively. In addition, IWOA can consistently provide a smaller SIAE value than its competitors for the three PV models, namely, the parameters extracted by IWOA are more accurate. The comparison also indicates that although the values of the parameters extracted by different methods are very close to each other, a small difference can have an impact on the performance of a PV model. The I-V and P-V characteristics corresponding to the extracted parameters of IWOA are plotted in Figs. 8–10 for the three PV models, respectively. It can be clearly seen that the calculated data are in very good agreement with the measured data throughout the whole range of voltage.

The above comparisons fully demonstrate that the proposed prey searching strategies can indeed enhance the performance of WOA

Table 3
Comparison of experimental results for the double diode model.

Method	Min	Max	Mean	Std. dev.
Rcr-IJADE [26]	9.824849E − 04	9.860244E − 04	9.826140E − 04	9.86E − 05
ABSO [29]	9.8344E − 04	NA	NA	NA
BBO-M [30]	9.8272E − 04	NA	NA	NA
IGHS [31]	9.8635E − 04	NA	NA	NA
SATLBO [34]	9.828037E − 04	1.047045E − 04	9.981111E − 04	1.951533E − 05
GOTLBO [35]	9.83177E − 04	1.78774E − 03	1.24360E − 03	2.09115E − 04
BMO [40]	9.8262E − 04	NA	NA	NA
CARO [42]	9.8260E − 04	NA	NA	NA
IJAYA [64]	9.8293E − 04	1.4055E − 03	1.0269E − 03	9.8625E − 05
PS [70]	1.5180E − 02	NA	NA	NA
SA [71]	1.9000E − 02	NA	NA	NA
MSSO [72]	9.8281E − 04	NA	NA	NA
CWOA [73]	9.8279E − 04	NA	NA	1.1333E − 07
WOA	1.1293E − 03	7.2449E − 03	3.3497E − 03	1.6685E − 03
CWOA	1.0968E − 03	2.8582E − 02	6.2915E − 03	6.8245E − 03
LWOA	1.0004E − 03	1.0942E − 02	3.8353E − 03	2.1608E − 03
PSO-WOA	1.1842E − 03	4.3031E − 03	2.7249E − 03	7.9163E − 04
IWOA	9.8255E − 04	1.0889E − 03	9.9693E − 04	1.9297E − 05

NA: Not available in the literature.

Table 4
Comparison of experimental results for the PV module model.

Method	Min	Max	Mean	Std. dev.
Rcr-IJADE [26]	2.425075E − 03	2.425075E − 03	2.425075E − 03	2.90E − 17
SATLBO [34]	2.425075E − 03	2.429130E − 03	2.425428E − 03	7.410517E − 07
CARO [42]	2.427E − 03	NA	NA	NA
IJAYA [64]	2.4251E − 03	2.4393E − 03	2.4289E − 03	3.7755E − 06
PS [70]	1.18E − 02	NA	NA	NA
SA [71]	2.70E − 03	NA	NA	NA
WOA	2.4407E − 03	2.6352E − 02	8.0251E − 03	6.8216E − 03
CWOA	2.5962E − 03	2.3216E − 01	3.9903E − 02	4.8032E − 02
LWOA	2.4529E − 03	9.2736E − 02	8.1755E − 03	1.4403E − 02
PSO-WOA	2.5313E − 03	3.8267E − 02	6.6495E − 03	6.8532E − 03
IWOA	2.4251E − 03	2.4335E − 03	2.4269E − 03	2.2364E − 06

NA: Not available in the literature.

Table 5
Comparison of the extracted parameters for the single diode model.

Method	I_{ph} (A)	I_{sd} (µA)	R_s (Ω)	R_{sh} (Ω)	n	RMSE
IADE [25]	0.7607	0.33613	0.03621	54.7643	1.4852	9.8900E − 04
Rcr-IJADE [26]	0.760776	0.323021	0.036377	53.718524	1.481184	9.860219E − 04
ABSO [29]	0.76080	0.30623	0.03659	52.2903	1.47583	9.9124E − 04
BBO-M [30]	0.76078	0.31874	0.03642	53.36277	1.47984	9.8634E − 04
GGHS [31]	0.76092	0.32620	0.03631	53.0647	1.48217	9.9079E − 04
SATLBO [34]	1.7608	0.32315	0.03638	53.7256	1.48123	9.8602E − 04
GOTLBO [35]	0.760780	0.331552	0.036265	54.115426	1.483820	9.8744E − 04
CARO [42]	0.76079	0.31724	0.03644	53.0893	1.48168	9.8665E − 04
IJAYA [64]	0.7608	0.3228	0.0364	53.7595	1.4811	9.8603E − 04
PS [70]	0.7617	0.9980	0.0313	64.1026	1.6000	2.863E − 01
SA [71]	0.7620	0.4798	0.0345	43.1034	1.5172	1.70E − 03
MSSO [72]	0.760777	0.323564	0.036370	53.742465	1.481244	9.8607E − 04
CWOA [73]	0.76077	0.3239	0.03636	63.7987	1.4812	9.8602E − 04
WOA	0.7606	0.3881	0.0357	60.5623	1.4999	1.0480E − 03
CWOA	0.7600	0.2831	0.0371	62.6183	1.4678	1.1812E − 03
LWOA	0.7602	0.4607	0.0350	75.4619	1.5177	1.2352E − 03
PSO-WOA	0.7597	0.3140	0.0366	58.8019	1.4783	1.1983E − 03
IWOA	0.7608	0.3232	0.0364	53.7317	1.4812	9.8602E − 04

considerably.

4.2.2. Convergence property

Convergence speed is an important criterion for measuring the performance of an optimization method. The convergence curves of the mean RMSE of WOA, CWOA, LWOA, PSO-WOA, and IWOA for the single diode, double diode, and PV module models are illustrated in Fig. 11. It is clearly observed that IWOA consistently converges much faster than other four methods throughout the whole evolutionary process on all three PV models. Although WOA, CWOA, and LWOA also converge fast in the beginning stage, they stagnate quickly and suffer from prematurity. PSO-WOA can converge continuously throughout the whole evolutionary process, but its speed is very slow. The comparison result indicates that IWOA is with the capability of breaking away from

Table 6
Comparison of the extracted parameters for the double diode model.

Method	I_{ph} (A)	I_{sd1} (µA)	R_s (Ω)	R_{sh} (Ω)	n_1	I_{sd2} (µA)	n_2	RMSE
Rcr-IJADE [26]	0.760781	0.225974	0.036740	55.485443	1.451017	0.749347	2.000000	9.824849E−04
ABSO [29]	0.76078	0.26713	0.03657	54.6219	1.46512	0.38191	1.98344	9.8344E−04
BBO-M [30]	0.76083	0.59115	0.03664	55.0494	2	0.24523	1.45798	9.8272E−04
IGHS [31]	0.76079	0.97310	0.03690	56.8368	1.92126	0.16791	1.42814	9.8635E−04
SATLBO [34]	0.76078	0.25093	0.03663	55.1170	1.45982	0.545418	1.99941	9.82804E−04
GOTLBO [35]	0.760752	0.800195	0.036783	56.075304	1.999973	0.220462	1.448974	9.83177E−04
BMO [40]	0.76078	0.21110	0.03682	55.8081	1.44533	0.87688	1.99997	9.8262E−04
CARO [42]	0.76075	0.29315	0.03641	54.3967	1.47338	0.09098	1.77321	9.8260E−04
IJAYA [64]	0.7601	0.0050445	0.0376	77.8519	1.2186	0.75094	1.6247	9.8293E−04
PS [70]	0.7602	0.9889	0.0320	81.3008	1.6000	0.0001	1.1920	1.5180E−02
SA [71]	0.7623	0.4767	0.0345	43.1034	1.5172	0.0100	2.0000	1.9000E−02
MSSO [72]	0.760748	0.234925	0.036688	55.714662	1.454255	0.671593	1.995305	9.8281E−04
CWOA [73]	0.76077	0.24150	0.03666	55.2016	1.45651	0.60000	1.9899	9.8272E−04
WOA	0.7611	0.3656	0.0354	55.5644	1.4970	0.1274	1.7961	1.1293E−03
CWOA	0.7613	0.1905	0.0359	50.0905	1.4564	0.2459	1.6065	1.0968E−03
LWOA	0.7608	0.1667	0.0361	55.2366	1.6086	0.2323	1.4658	1.0004E−03
PSO-WOA	0.7604	0.1079	0.0367	74.3924	1.4072	0.6665	1.7141	1.1842E−03
IWOA	0.7608	0.6771	0.0367	55.4082	2.0000	0.2355	1.4545	9.8255E−04

Table 7
Comparison of the extracted parameters for the PV module model.

Method	I_{ph} (A)	I_{sd} (µA)	R_s (Ω)	R_{sh} (Ω)	n	RMSE
Rcr-IJADE [26]	1.030514	3.482263	1.201271	981.982240	48.642835	2.425075E−03
SATLBO [34]	1.030511	3.48271	1.201263	982.40376	48.6433077	2.425075E−03
CARO [42]	1.03185	3.28401	1.20556	841.3213	48.40363	2.427E−03
EHA-NMS [51]	1.030514	3.482263	1.201271	981.982256	48.642835	2.425E−04
IJAYA [64]	1.0305	3.4703	1.2016	977.3752	48.6298	2.4251E−03
PS [70]	1.0313	3.1756	1.2053	714.2857	48.2889	1.18E−02
SA [71]	1.0331	3.6642	1.1989	833.3333	48.8211	2.7000E−03
WOA	1.0309	3.4375	1.1994	921.7861	48.5958	2.4407E−03
CWOA	1.0272	4.2334	1.1879	1923.9615	49.3908	2.5962E−03
LWOA	1.0293	3.6916	1.1985	1198.7830	48.8626	2.4529E−03
PSO-WOA	1.0301	3.6169	1.1900	965.9555	48.7927	2.5313E−03
IWOA	1.0305	3.4717	1.2016	978.6771	48.6313	2.4251E−03

the adsorption of local minima and of finding a more promising searching direction. Namely, it is able to achieve a stronger equilibrium between the local exploitation and global exploration.

4.2.3. Robustness

Population-based algorithms essentially possess random characteristic owing to the randomly initialized population and randomization procedures. Thus, a number of independent runs with different initial populations can be conducted to validate their stability and consistency, i.e., robustness performance. The standard deviation results over 50 independent runs tabulated in Tables 2–4 clearly illustrate that the recorded results of IWOA are significantly smaller than those of WOA, CWOA, LWOA, and PSO-WOA on all three PV models. In addition, when compared with other recently-developed methods, IWOA also performs highly competitively. The comparison results demonstrate that IWOA possesses good robustness.

4.2.4. Statistical analysis

The significance difference between two methods can be measured by the statistical analysis. In this paper, on one hand, the Wilcoxon's rank sum test at 0.05 confidence level is used to show the significance difference between IWOA and the involved WOA based methods on the same PV model. Wilcoxon's test is a simple, yet safe and robust non-parametric test for paired statistical comparisons when samples are independent and it is popular in evolutionary computing. The result based on the Wilcoxon's rank sum test is summarized in Table 11. The mark "†" denotes that IWOA is statistically better than its competitor. The result manifests again that IWOA significantly outperforms WOA,

IWOA, CWOA, and PSO-WOA on all three PV models. Namely, for each PV model, IWOA achieves more promising results than its competitors above the 95% probability level in 50 independent runs. On the other hand, the Friedman test is performed to obtain the rankings of different methods for all three PV models. It is a non-parametric statistical test used to detect differences in treatments across multiple test attempts. The result based on the Friedman test tabulated in Table 12 clearly shows that IWOA achieves the best rank, followed by PSO-WOA, WOA, LWOA, and CWOA.

The comparison results further demonstrate that IWOA exhibits the best performance on all three benchmark test PV models from the perspective of statistical analysis. It is with the capability of achieving overall higher quality of the final solutions and the proposed prey searching strategies can indeed significantly enhance the performance of WOA.

4.3. Experimental results on practical PV power stations

In the previous section, the effectiveness of IWOA is validated on three benchmark test PV models. To further verify IWOA, in this section, two PV power station models with more modules/panels in the Guizhou Power Grid of China are employed. Both models are constructed in MATLAB/Simulink to generate the simulated *I-V* data. The search ranges of the involved parameters for both PV models are tabulated in Table 13.

4.3.1. Experimental results on the EMZ PV power station model

The first model is the EMZ PV power station model. The installed

Table 8
Sum of individual absolute error (SIAE) based on the extracted parameters for the single diode model.

| Item	V_L (V)	I_L measured (A)	I_L calculated (A)									
			Rcr−LJADE [26]	ABSO [29]	BBO−M [30]	CARO [42]	IJAYA [64]	WOA	CWOA	LWOA	PSO−WOA	IWOA
1	−0.2057	0.7640	0.764009559	0.764201	0.764006	0.764023	0.76408300	0.76356605	0.76284472	0.762257556	0.76268147	0.76408652
2	−0.1291	0.7620	0.76266611	0.762737	0.762604	0.762610	0.76265947	0.76230195	0.76162214	0.76156092	0.76137957	0.76266187
3	−0.0588	0.7605	0.761135473	0.761393	0.761317	0.761313	0.76135269	0.76114171	0.76050002	0.76062959	0.76018466	0.76135428
4	0.0057	0.7605	0.76014966	0.76016	0.760135	0.760121	0.76015229	0.76007662	0.75947005	0.75977445	0.75908786	0.76015409
5	0.0646	0.7600	0.75905702	0.759032	0.759053	0.759031	0.75905435	0.75910167	0.75852762	0.75899090	0.75808427	0.75905604
6	0.1185	0.7590	0.75804472	0.757992	0.758056	0.758026	0.75804225	0.75820105	0.75765824	0.75826449	0.75715847	0.75804369
7	0.1678	0.7570	0.75709510	0.757017	0.757120	0.757082	0.75709227	0.75734918	0.75683904	0.75756932	0.75628646	0.75709215
8	0.2132	0.7570	0.75615050	0.756047	0.756182	0.756139	0.75614266	0.75648551	0.75601534	0.75684368	0.75541118	0.75614282
9	0.2545	0.7555	0.75508177	0.754977	0.755138	0.755091	0.75508882	0.75549572	0.75508296	0.75596612	0.75442568	0.75508821
10	0.2924	0.7540	0.75367033	0.753547	0.753723	0.753674	0.75366651	0.75410735	0.75378706	0.75465539	0.75306950	0.75366542
11	0.3269	0.7505	0.751139542	0.751277	0.751453	0.751408	0.75139433	0.75182020	0.75164959	0.75239658	0.75085872	0.75138897
12	0.3585	0.7465	0.74735737	0.74726	0.747414	0.747378	0.74735805	0.74770861	0.74776847	0.74824841	0.74688562	0.74734907
13	0.3873	0.7385	0.74010420	0.740051	0.740168	0.740149	0.74012235	0.74031430	0.74069358	0.74074194	0.73970129	0.74009725
14	0.4137	0.7280	0.72740088	0.727411	0.727416	0.727421	0.72738829	0.72740647	0.72817201	0.72765015	0.72706565	0.72739665
15	0.4373	0.7065	0.70694631	0.707033	0.706985	0.707016	0.70697944	0.70673108	0.70786686	0.70675469	0.70667461	0.70695260
16	0.4590	0.6755	0.67530400	0.675431	0.675269	0.675325	0.67528720	0.67487104	0.67625883	0.67468728	0.67504810	0.67529377
17	0.4784	0.6320	0.63089105	0.631046	0.630728	0.630799	0.63076483	0.63035869	0.63176746	0.63004594	0.63064089	0.63088297
18	0.4960	0.5730	0.57208973	0.57223	0.571887	0.571959	0.57193362	0.57158761	0.57274947	0.57125856	0.57181580	0.57208084
19	0.5119	0.4990	0.49949902	0.499591	0.499563	0.499622	0.49961038	0.49914891	0.49985154	0.49891195	0.49918854	0.49949084
20	0.5265	0.4130	0.41349030	0.413524	0.413612	0.413646	0.41364992	0.41337251	0.41352267	0.41329610	0.41315714	0.41349340
21	0.5398	0.3165	0.31721532	0.317184	0.317485	0.317192	0.31750930	0.31731762	0.31697496	0.31740962	0.31687154	0.31721981
22	0.5521	0.2120	0.21210468	0.212023	0.212142	0.212126	0.21215297	0.21235602	0.21170017	0.21256927	0.21177887	0.21210387
23	0.5633	0.1035	0.10271603	0.10263	0.102245	0.102621	0.10224948	0.10301807	0.10231134	0.10326296	0.10246167	0.10272213
24	0.5736	−0.0100	−0.00924563	−0.00931	−0.008731	−0.009415	−0.00871730	−0.00903746	−0.00950796	−0.00886959	−0.00940270	−0.00924825
25	0.5833	−0.1230	−0.12437754	−0.12438	−0.125537	−0.124350	−0.12550357	−0.12439248	−0.12433268	−0.12441932	−0.12438849	−0.12438143
26	0.5900	−0.2100	−0.20919680	−0.20911	−0.208530	−0.209138	−0.20846403	−0.20945119	−0.20882732	−0.20906970	−0.20906970	−0.20919380
SIAE			0.01770357	0.017748	0.021313	0.018155	0.02151611	0.01840477	0.02088032	0.02226519	0.02267343	0.01770338

Table 9
Sum of individual absolute error (SIAE) based on the extracted parameters for the double diode model.

Item	V_L (V)	I_L measured (A)	I_L calculated (A)									
			Rcr-IJADE [26]	ABSO [29]	BBO-M [30]	CARO [42]	IJAYA [64]	WOA	CWOA	LWOA	PSO-WOA	IWOA
1	−0.2057	0.7640	0.76409268	0.764031	0.764012	0.764026	0.76403108	0.76430787	0.76484710	0.76404413	0.76273996	0.76398588
2	−0.1291	0.7620	0.76265394	0.762629	0.762622	0.762619	0.76264510	0.76293013	0.76331893	0.76265825	0.76171072	0.76260424
3	−0.0588	0.7605	0.76135755	0.761343	0.761345	0.761328	0.76137259	0.76166555	0.76191631	0.76138623	0.76076591	0.76133595
4	0.0057	0.7605	0.76016253	0.760162	0.760172	0.760141	0.76020309	0.76050464	0.76062879	0.76021858	0.75989805	0.76017130
5	0.0646	0.7600	0.75906000	0.75908	0.759098	0.759056	0.75913193	0.75944186	0.75945060	0.75914997	0.75910202	0.75910440
6	0.1185	0.7590	0.75805065	0.758081	0.758106	0.758055	0.75814115	0.75846007	0.75836372	0.75816376	0.75836214	0.75811760
7	0.1678	0.7570	0.75709635	0.757139	0.757168	0.757114	0.75720437	0.75753206	0.75734104	0.75723410	0.75765051	0.75718346
8	0.2132	0.7570	0.75614465	0.756193	0.756221	0.756171	0.75625597	0.75659448	0.75631980	0.75630052	0.75690347	0.75624008
9	0.2545	0.7555	0.75508115	0.755132	0.755157	0.755121	0.75518696	0.75553061	0.75518749	0.75525168	0.75599908	0.75517574
10	0.2924	0.7540	0.75366874	0.753694	0.753708	0.753696	0.75373008	0.75406336	0.75367252	0.75381935	0.75465953	0.75372465
11	0.3269	0.7505	0.75139511	0.751392	0.751395	0.751418	0.75140585	0.75168958	0.75128154	0.75151173	0.75238137	0.75140265
12	0.3585	0.7465	0.74734939	0.747322	0.747310	0.747370	0.74730817	0.74748201	0.74709861	0.74741355	0.74824273	0.74730729
13	0.3873	0.7385	0.74010214	0.740044	0.740029	0.740121	0.74001849	0.73998757	0.73967977	0.74007617	0.74079653	0.74000499
14	0.4137	0.7280	0.72738784	0.727331	0.727270	0.727373	0.72725674	0.72698845	0.72680735	0.72727119	0.72782521	0.72727690
15	0.4373	0.7065	0.70695162	0.706896	0.706869	0.706955	0.70686230	0.70625467	0.70622899	0.70672751	0.70708227	0.70684158
16	0.4590	0.6755	0.67530112	0.675265	0.675217	0.675261	0.67522394	0.67439188	0.67451681	0.67499970	0.67513836	0.67522637
17	0.4784	0.6320	0.63088766	0.630889	0.630753	0.630744	0.63077352	0.62994708	0.63016945	0.63057698	0.63050636	0.63087498
18	0.4960	0.5730	0.57207477	0.572114	0.571976	0.571923	0.57200430	0.57130765	0.57154658	0.57182629	0.57156446	0.57212299
19	0.5119	0.4990	0.49949417	0.499533	0.499685	0.499610	0.49971050	0.49903659	0.49921149	0.49933619	0.49891653	0.49955490
20	0.5265	0.4130	0.41349125	0.413525	0.413723	0.413658	0.41373174	0.41342718	0.41348536	0.41345886	0.41292926	0.41354760
21	0.5398	0.3165	0.31721918	0.31723	0.317553	0.317521	0.31753942	0.31749922	0.31743277	0.31729155	0.31671849	0.31724247
22	0.5521	0.2120	0.21210831	0.21209	0.212151	0.212162	0.21211485	0.21259816	0.21244113	0.21224241	0.21170555	0.21208993
23	0.5633	0.1035	0.10272032	0.102694	0.102208	0.102753	0.10215958	0.10323976	0.10305914	0.10287125	0.10245567	0.10268378
24	0.5736	−0.0100	−0.00924461	−0.00927	−0.008750	−0.009278	−0.00878197	−0.00891778	−0.00903964	−0.00914905	−0.00935990	−0.00928723
25	0.5833	−0.1230	−0.12437667	−0.12439	−0.125513	−0.124355	−0.12551336	−0.12445451	−0.12442746	−0.12439317	−0.12431581	−0.12438984
26	0.5900	−0.2100	−0.20919499	−0.20917	−0.208379	−0.209207	−0.20831777	−0.20969188	−0.20949928	−0.20932279	−0.20898664	−0.20915789
SIAE			0.01770933	0.017489	0.021360	0.018478	0.02129082	0.01947347	0.02024892	0.01785274	0.02050791	0.01735511

Table 10
Sum of individual absolute error (SIAE) based on the extracted parameters for the PV module model.

Item	V_L (V)	I_L measured (A)	I_L calculated (A)							
			Rcr-IJADE [26]	EHA-NMS [51]	IJAYA [64]	WOA	CWOA	LWOA	PSO-WOA	IWOA
1	0.1248	1.0315	1.02912049	1.02912209	1.02912228	1.02943791	1.02651308	1.02811508	1.02870266	1.02913532
2	1.8093	1.0300	1.02738564	1.02738435	1.02737617	1.02758792	1.02560903	1.02668496	1.02693520	1.02739106
3	3.3511	1.0260	1.02573499	1.02574214	1.02572968	1.02584421	1.02472425	1.02532317	1.02526574	1.02574369
4	4.7622	1.0220	1.02409557	1.02410399	1.02408866	1.02411439	1.02376495	1.02393737	1.02360107	1.02410103
5	6.0538	1.0180	1.02227575	1.02228341	1.02226793	1.02221253	1.02253685	1.02233900	1.02175348	1.02227671
6	7.2364	1.0155	1.01991719	1.01991740	1.01990268	1.01977720	1.02066097	1.02016028	1.01935883	1.01990797
7	8.3189	1.0140	1.01635389	1.01635081	1.01633264	1.01615627	1.01745730	1.01673816	1.01576192	1.01634000
8	9.3097	1.0100	1.01048191	1.01049143	1.01046533	1.01026202	1.01180401	1.01097037	1.00987330	1.01048094
9	10.2163	1.0035	1.00068707	1.00067876	1.00060024	1.00043953	1.00201526	1.00118677	1.00004046	1.00067050
10	11.0449	0.9880	0.98465514	0.98465335	0.98452419	0.98443459	0.98582572	0.98512336	0.98401865	0.98464912
11	11.8018	0.9630	0.95969425	0.95969741	0.95950393	0.95953190	0.96054672	0.96006841	0.95910985	0.95969846
12	12.4929	0.9255	0.92305160	0.92304875	0.92282835	0.92296526	0.92348504	0.92327833	0.92256965	0.92305447
13	13.1231	0.8725	0.87258829	0.87258816	0.87259590	0.87260564	0.87261371	0.87266445	0.87228160	0.87259742
14	13.6983	0.8075	0.80731392	0.80731012	0.80727526	0.80743131	0.80701512	0.80725146	0.80722624	0.80732062
15	14.2221	0.7265	0.72796294	0.72795782	0.72833977	0.72816825	0.72748045	0.72780412	0.72811018	0.72796714
16	14.6995	0.6345	0.63646347	0.63646618	0.63714108	0.63673901	0.63594580	0.63626478	0.63682685	0.63647300
17	15.1346	0.5345	0.53569189	0.53569607	0.53621404	0.53599662	0.53523796	0.53548798	0.53620045	0.53569869
18	15.5311	0.4275	0.42882216	0.42881615	0.42950971	0.42911092	0.42848144	0.42863256	0.42938030	0.42881530
19	15.8929	0.3185	0.31867170	0.31866866	0.31877043	0.31892722	0.31847644	0.31852785	0.31920232	0.31866501
20	16.2229	0.2085	0.20785189	0.20785711	0.20738439	0.20805509	0.20779651	0.20776740	0.20827584	0.20785201
21	16.5241	0.1010	0.09835838	0.09835421	0.09616244	0.09847325	0.09839638	0.09831655	0.09858551	0.09834902
22	16.7987	−0.0080	−0.00817367	−0.00816934	−0.00832566	−0.00814173	−0.00806137	−0.00815848	−0.00818287	−0.00817323
23	17.0499	−0.1110	−0.11096908	−0.11096846	−0.11093079	−0.11104067	−0.11083318	−0.11091523	−0.11127065	−0.11097018
24	17.2793	−0.2090	−0.20912100	−0.20911762	−0.20923354	−0.20929371	−0.20899077	−0.20902888	−0.20973822	−0.20911611
25	17.4885	−0.3030	−0.30202427	−0.30202238	−0.30083914	−0.30230345	−0.30193505	−0.30190522	−0.30297927	−0.30201694
SIAE			0.04177271	0.04178790	0.04891051	0.04204177	0.04488229	0.04277834	0.04452318	0.04176116
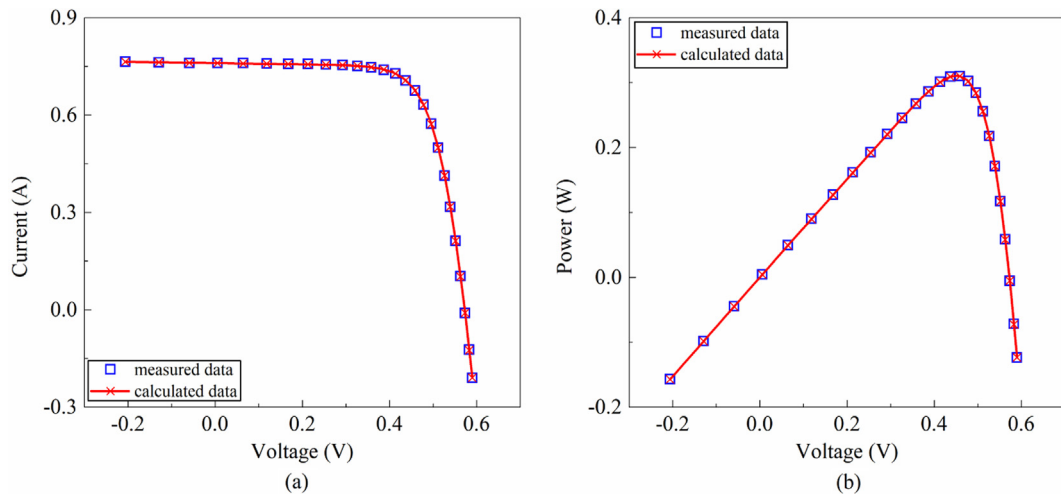
Fig. 8. Comparison of the measured data and calculated data obtained by IWOA for the single diode model. (a) *I-V* characteristics. (b) *P-V* characteristics.
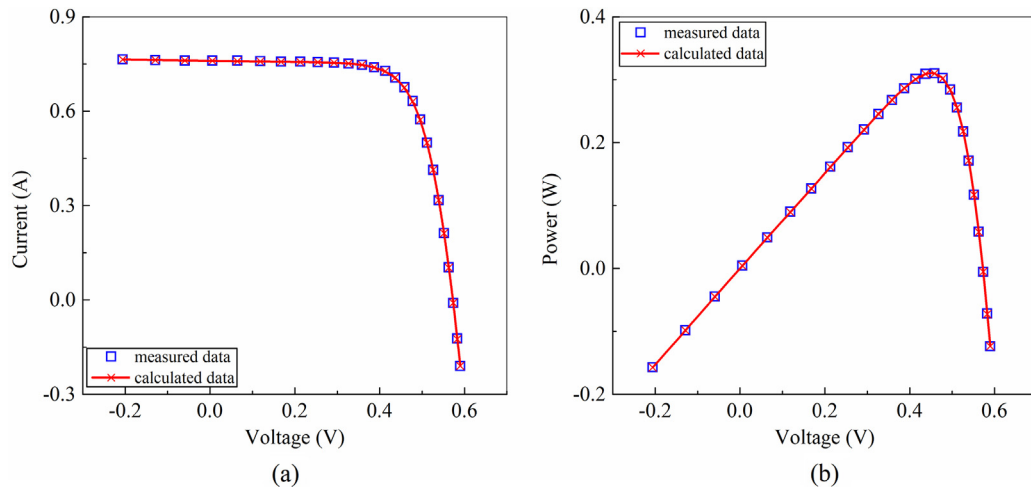
Fig. 9. Comparison of the measured data and calculated data obtained by IWOA for the double diode model. (a) *I-V* characteristics. (b) *P-V* characteristics.
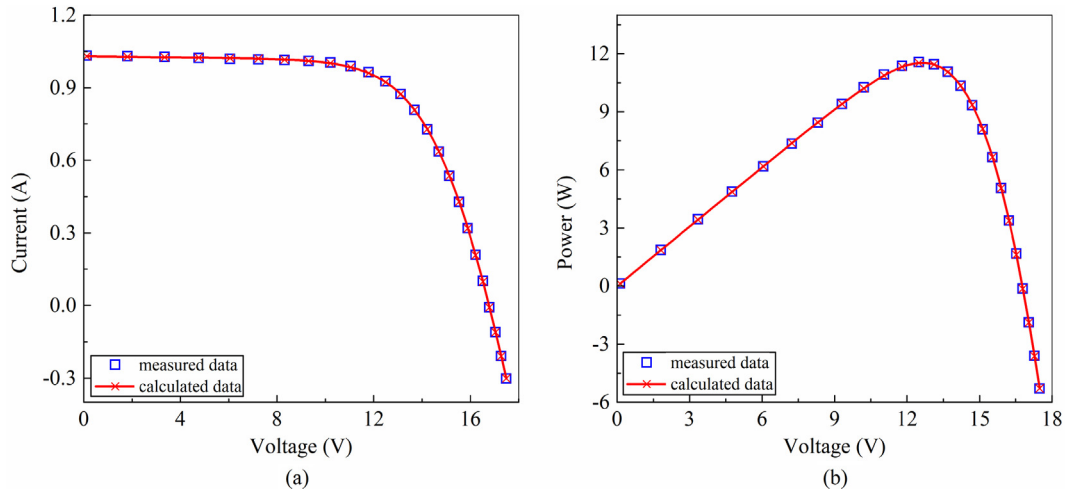
Fig. 10. Comparison of the measured data and calculated data obtained by IWOA for the PV module model. (a) *I-V* characteristics. (b) *P-V* characteristics.
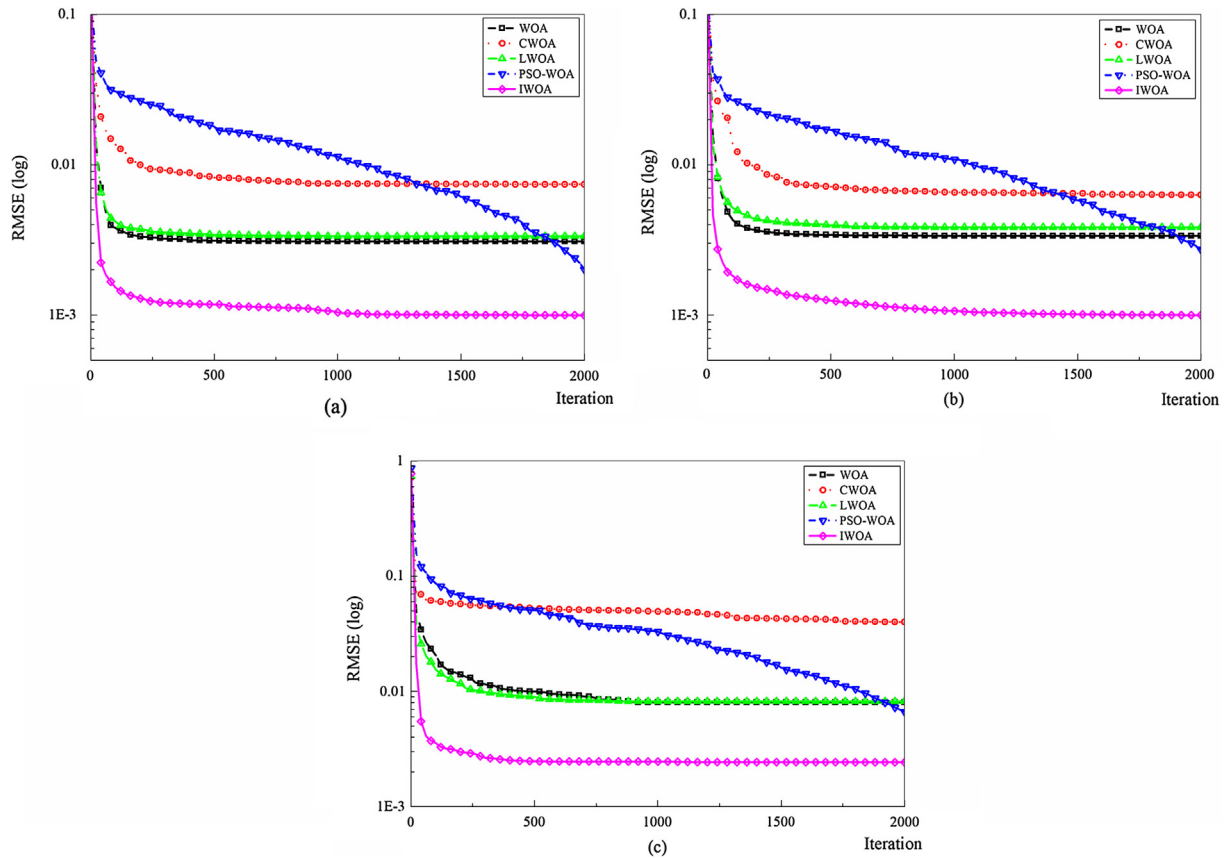

Fig. 11. Convergence curves of involved methods. (a) single diode model. (b) double diode model. (c) PV module model.

Table 11
Statistical results based on the Wilcoxon's rank sum test for the three benchmark test PV models.

IWOA vs.	WOA	CWOA	LWOA	PSO-WOA
Single diode model	†	†	†	†
Double diode model	†	†	†	†
PV module model	†	†	†	†

capacity of this power station is 50 MW. Each inverter in the power station contains eight PV strings in parallel and each string is composed of 18 PV panels in series. This power station has three types of PV panels, i.e., CS6U-320, -325, -330P (Canadian Solar). Each panel consists of 72 (4 × 18 connected in parallel and in series, respectively) poly-crystalline cells. In this subsection, the involved parameters associated with a CS6U-320P based string operating under 670 W/m² at 21 °C with 50 *I-V* data points are extracted. The RMSE values of different methods are summarized in Table 14. It is clear that IWOA performs significantly better than all of the other methods in terms of the minimum, maximum, and mean RMSE values, which is also supported by the Wilcoxon's test results. According to the standard deviation values, IWOA provides the smallest value, meaning that IWOA is the most robust one among the five methods. The extracted values for

Method	Ranking
WOA	3.0
CWOA	5.0
LWOA	4.0
PSO-WOA	2.0
IWOA	1.0

Table 13
Search range of parameters for the simulated data.

Parameter	Lower bound	Upper bound
I_{ph} (A)	0	10
I_{sd} (μA)	0	50
R_s (Ω)	0	2
R_{sh} (MΩ)	0	1
n	1	50

the relevant parameters are listed in Table 15. By utilizing the extracted parameters, the *I-V* and *P-V* characteristic curves are reconstructed as shown in Fig. 12. It clearly demonstrates that the calculated data ob-

tained by IWOA fit the simulated data very well. The SIAE values presented in Table 15 manifest that IWOA obtains the smallest value, which indicates that IWOA extracts the highest accuracy of the parameters for the EMZ PV string model. In addition, the convergence curves in Fig. 13 reveal that IWOA is significantly faster than other methods throughout the whole evolutionary process.

4.3.2. Experimental results on the YL PV power station model

Another model is the YL PV power station model. The installed capacity of this power station is also 50 MW. In this power station, each inverter is also composed of eight PV strings in parallel. Each PV string consists of 2×11 PV panels connected in parallel and in series, respectively. This power station has only one type of PV panel, i.e., JAM6-60-295W-4BB (JA Solar) which consists of 60 (3×20 connected in parallel and in series, respectively) mono-crystalline cells. In this sub-section, the involved parameters associated with a string operating under 750 W/m² at 23 °C with 50 *I-V* data points are extracted. The experimental results are presented in Tables 16, 17, and in Figs. 14 and 15. Similar to the comparison results on the EMZ PV power station model, IWOA achieves the best results in terms of RMSE values, SIAE value, and convergence speed.

All in all, it can be seen that IWOA performs highly competitively and is very effective in extracting unknown parameters of practical PV power station models. In addition, through comparison of the experimental results on the benchmark test PV models and the practical PV

Table 14
Comparison of experimental results for the EMZ PV power station model.

Method	Min	Max	Mean	Std. dev.	Wilcoxon's test
WOA	6.9583E−03	2.3717E−01	9.5948E−02	6.2571E−02	†
CWOA	3.9792E−02	1.7923E+00	9.3280E−01	6.4454E−01	†
LWOA	8.9479E−03	1.8379E−01	9.6972E−02	4.8196E−02	†
PSO-WOA	8.7610E−03	3.1456E−01	1.5429E−01	6.8930E−02	†
IWOA	8.7102E−04	1.8345E−02	1.4223E−02	3.7765E−03	

Table 15
Comparison of the extracted parameters for the EMZ PV power station model.

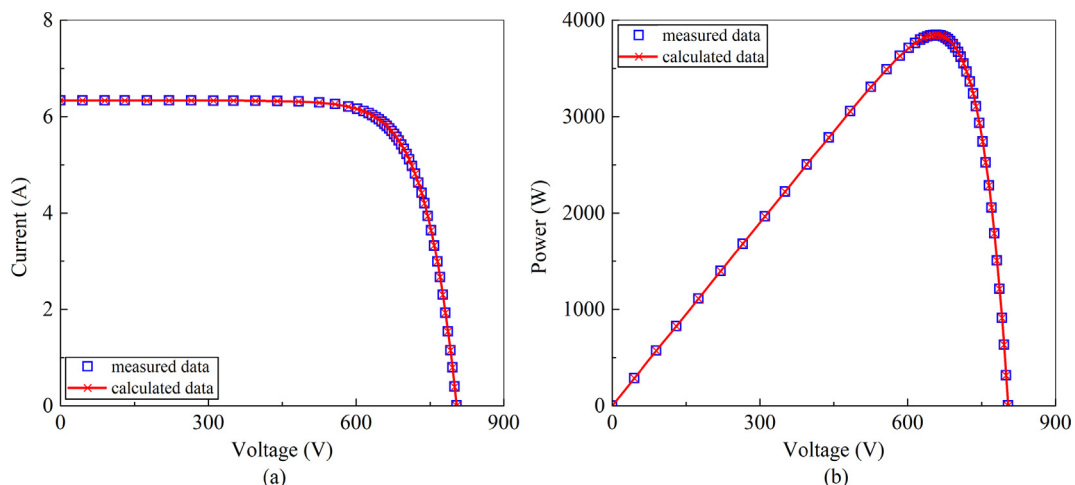| Method	I_{ph} (A)	I_{sd} (μA)	R_s (Ω)	R_{sh} (MΩ)	n	RMSE	SIAE
WOA	1.5823	0.2694	0.0261	0.0333	6.2819	6.9583E−03	2.7480E−01
CWOA	1.5959	2.4931	0.0036	0.1980	7.3225	3.9792E−02	1.8037E+00
LWOA	1.5801	0.2431	0.0259	0.2153	6.2406	8.9479E−03	3.9367E−01
PSO-WOA	1.5839	0.4830	0.0200	0.1409	6.5236	8.7610E−03	3.6833E−01
IWOA	1.5831	0.4114	0.0211	0.6986	6.4559	8.7102E−04	3.7927E−02

Fig. 12. Comparison of the measured data and calculated data obtained by IWOA for the EMZ PV power station model. (a) *I-V* characteristics. (b) *P-V* characteristics.
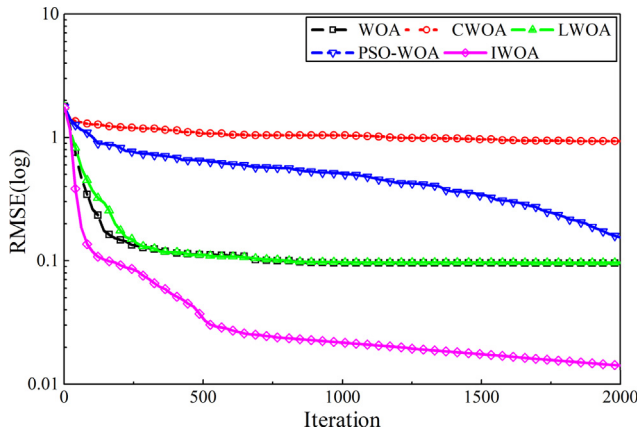
Fig. 13. Convergence curves of involved methods for the EMZ PV power station model.

Fig. 15. Convergence curves of involved methods for the YL PV power station model.

power station models, it can be summarized that the more panels the PV model contains, the more performance superiority the proposed IWOA has over WOA, CWOA, LWOA, and PSO-WOA, which indicates that IWOA is a promising alternative for large-scale PV models with a large number of panels.

5. Conclusions and future work

In this paper, an improved whale optimization algorithm named IWOA is proposed to accurately extract the parameters of different PV models. In IWOA, two prey searching strategies are proposed to enhance the performance of the original WOA. The experimental results of three benchmark test PV models and two practical PV power station

Table 16
Comparison of experimental results for the YL PV power station model.

Method	Min	Max	Mean	Std. dev.	Wilcoxon's test
WOA	$2.2661E-02$	$2.3973E-01$	$1.0031E-01$	$5.5273E-02$	†
CWOA	$3.3622E-02$	$2.1704E+00$	$1.5351E+00$	$7.9203E-01$	†
LWOA	$1.0145E-02$	$2.2156E-01$	$9.5831E-02$	$5.9962E-02$	†
PSO-WOA	$2.4959E-02$	$4.8968E-01$	$1.9973E-01$	$1.1013E-01$	†
IWOA	$2.6025E-04$	$2.2631E-02$	$1.6528E-02$	$4.6145E-03$	

Table 17
Comparison of the extracted parameters for the YL PV power station model.

Method	I_{ph} (A)	I_{sd} (µA)	R_s (Ω)	R_{sh} (MΩ)	n	RMSE	SIAE
WOA	2.5517	2.0280	0.0041	0.0525	5.4631	$2.2661E-02$	$2.0607E+00$
CWOA	2.5453	2.7804	0.0006	0.0585	5.5875	$3.3622E-02$	$2.8232E+00$
LWOA	2.5415	0.7845	0.0086	0.0745	5.1185	$1.0145E-02$	$6.5016E-01$
PSO-WOA	2.5482	1.8054	0.0055	0.6393	5.4207	$2.4959E-02$	$2.1942E+00$
IWOA	2.5425	0.6790	0.0103	0.0032	5.0713	$2.6025E-04$	$2.1171E-02$
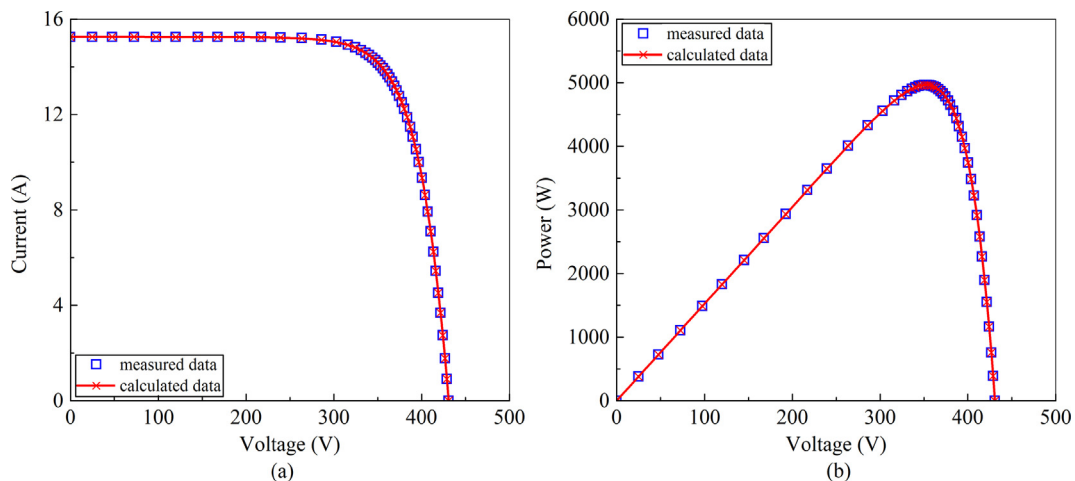
Fig. 14. Comparison of the measured data and calculated data obtained by IWOA for the YL PV power station model. (a) *I-V* characteristics. (b) *P-V* characteristics.

models in the Guizhou Power Grid of China in terms of the final solution quality, convergence speed, robustness, and statistics comprehensively demonstrate that IWOA, benefited from the proposed two prey searching strategies, is with the strong capability of highly balancing the local exploitation ability and global exploration ability. They are also better than those of other three advanced variants of WOA and some recently-developed parameter extraction methods. In short, it can be used as a promising alternative for parameter extraction problem of PV models.

IWOA has proven itself a promising method. In future work, we will investigate parameter adaptive methods to effectively adjust the coefficient A to further enhance the performance of IWOA.

Appendix A

Algorithm 1:The main procedure of WOA
1: Generate a random initial population$X$
2: Evaluate the fitness of each individual
3 Select the best individual X_s^0 asX_g
4 Initialize the iteration counter$t = 1$
5: **While** the stopping condition is not satisfied **do**
6:   **for** $i = 1$ to ps **do**
7:   Update A, C, b, l, and$p$
8:   **for** $d = 1$ to D **do**
9:   **if** $p < 0.5$ **then**
10:   **if** $\|A\| \geqslant 1$ **then**
11:   Select a random individualX_r^t
12: $S = \|C \cdot x_{r,d}^t - x_{i,d}^t\|$
13: $x_{i,d}^{t+1} = x_{r,d}^t - A \cdot S$
14:   **else**
15: $S = \|C \cdot x_{g,d} - x_{i,d}^t\|$
16: $x_{i,d}^{t+1} = x_{g,d} - A \cdot S$
17:   **end if**
18:   **else**
19: $S' = \|x_{g,d} - x_{i,d}^t\|$
20: $x_{i,d}^{t+1} = S' \cdot \exp(bl) \cdot \cos(2\pi l) + x_{g,d}$
21:   **end if**
22:   **end for**
23:   **end for**
24:   Evaluate the fitness of each individual
25:   Select the best individual X_s^{t+1} of the current iteration
26:   **if** $f(X_s^{t+1}) < f(X_g)$ **then**
27:   Replace X_g withX_s^{t+1}
28:   **end if**
29: $t = t + 1$
30: **End while**

Appendix B

Algorithm 2:The main procedure of IWOA
1: Generate a random initial population$X$
2: Evaluate the fitness of each individual
3 Select the best individual X_s^0 asX_g
4 Initialize the iteration counter$t = 1$
5: **While** the stopping condition is not satisfied **do**
6:   **for** $i = 1$ to ps **do**
7:   Update A, C, b, l, and$p$
8:   **for** $d = 1$ to D **do**
9:   **if** $p < 0.5$ **then**

10:	**if** $|A| \geqslant 1$ **then**
11:	Select a random individual X_{r1}^t
12:	$S = |x_{i,d}^t - x_{r1,d}^t|$
13:	$x_{i,d}^{t+1} = x_{r1,d}^t - A \cdot S$
14:	**else**
15:	Select a random individual X_{r2}^t
16:	$S = |x_{g,d} - x_{r2,d}^t|$
17:	$x_{i,d}^{t+1} = x_{r2,d}^t - A \cdot S$
18:	**end if**
19:	**else**
20:	$S' = |x_{gd} - x_{id}^t|$
21:	$x_{id}^{t+1} = S' \cdot \exp(bl) \cdot \cos(2\pi l) + x_{gd}$
22:	**end if**
23:	**end for**
24:	**end for**
25:	Evaluate the fitness of each individual
26:	Select the best individual X_s^{t+1} of the current iteration
27:	**if** $f(X_s^{t+1}) < f(X_g)$ **then**
28:	Replace X_g with X_s^{t+1}
29:	**end if**
30:	$t = t + 1$
31:	**End while**

References

[1] Malinowski M, Leon JI, Abu-Rub H. Solar photovoltaic and thermal energy systems: current technology and future trends. P IEEE 2017;105:2132–46.
[2] China Energy Net. [Online]. Available: <http://www.china5e.com>.
[3] Chin VJ, Salam Z, Ishaque K. Cell modelling and model parameters estimation techniques for photovoltaic simulator application: a review. Appl Energ 2015;154:500–19.
[4] Jordehi AR. Parameter estimation of solar photovoltaic (PV) cells: a review. Renew Sust Energ Rev 2016;61:354–71.
[5] Youssef A, El-Telbany M, Zekry A. The role of artificial intelligence in photo-voltaic systems design and control: a review. Renew Sust Energ Rev 2017;78:72–9.
[6] Gomes RCM, Vitorino MA, Fernandes DA, Wang R. Shuffled complex evolution on photovoltaic parameter extraction: a comparative analysis. IEEE Trans Sustain Energ 2016;8:805–15.
[7] Brano VL, Ciulla G. An efficient analytical approach for obtaining a five parameters model of photovoltaic modules using only reference data. Appl Energ 2013;111:894–903.
[8] Louzazni M, Aroudam EH. An analytical mathematical modeling to extract the parameters of solar cell from implicit equation to explicit form. Appl Solar Energy 2015;51:165–71.
[9] Batzelis EI, Papathanassiou SA. A method for the analytical extraction of the single-diode PV model parameters. IEEE Trans Sustain Energ 2016;7:504–12.
[10] Wolf P, Benda V. Identification of PV solar cells and modules parameters by combining statistical and analytical methods. Sol Energy 2013;93:151–7.
[11] Orioli A, Gangi AD. A procedure to calculate the five-parameter model of crystalline silicon photovoltaic modules on the basis of the tabular performance data. Appl Energ 2013;102:1160–77.
[12] Saleem H, Karmalkar S. An analytical method to extract the physical parameters of a solar cell from four points on the illuminated J-V curve. IEEE Elect Device L 2009;30:349–52.
[13] Khan F, Baek S, Kim JH. Wide range temperature dependence of analytical photovoltaic cell parameters for silicon solar cells under high illumination conditions. Appl Energ 2016;183:715–24.
[14] Miceli R, Orioli A, Di Gangi A. A procedure to calculate the I-V characteristics of thin-film photovoltaic modules using an explicit rational form. Appl Energ 2015;155:613–28.
[15] Wang G, Zhao K, Shi J, Chen W, Zhang H, Yang X, et al. An iterative approach for modeling photovoltaic modules without implicit equations. Appl Energ 2017;202:189–98.
[16] Bana S, Saini RP. Identification of unknown parameters of a single diode photovoltaic model using particle swarm optimization with binary constraints. Renew Energ 2017;101:1299–310.
[17] Li W, Paul MC, Rolley M, Sweet T, Gao M, Siviter J, et al. A scaling law for monocrystalline PV/T modules with CCPC and comparison with triple junction PV cells. Appl Energ 2017;202:755–71.
[18] Gao X, Cui Y, Hu J, Xu G, Yu Y. Lambert W-function based exact representation for double diode model of solar cells: comparison on fitness and parameter extraction. Energ Convers Manage 2016;127:443–60.
[19] Villalva MG, Gazoli JR, Filho ER. Comprehensive approach to modeling and simulation of photovoltaic arrays. IEEE Trans Power Elect 2009;24:1198–208.
[20] Bastidasrodriguez JD, Petrone G, Ramospaja CA, Spagnuolo G. A genetic algorithm for identifying the single diode model parameters of a photovoltaic panel. Math Comput Simul 2017;131:38–54.
[21] Zagrouba M, Sellami A, Bouaicha M, Ksouri M. Identification of PV solar cells and modules parameters using the genetic algorithms: application to maximum power extraction. Sol Energy 2010;84:860–6.
[22] Soon JJ, Low KS. Photovoltaic model identification using particle swarm optimization with inverse barrier constraint. IEEE Trans Power Elect 2012;27:3975–83.
[23] Jordehi AR. Time varying acceleration coefficients particle swarm optimisation (TVACPSO): a new optimisation algorithm for estimating parameters of PV cells and modules. Energ Convers Manage 2016;129:262–74.
[24] Nunes HGG, Pombo JAN, Mariano SJPS, Calado MRA, Felippe De Souza JAM. A new high performance method for determining the parameters of PV cells and modules based on guaranteed convergence particle swarm optimization. Appl Energ 2018;211:774–91.
[25] Jiang LL, Maskell DL, Patra JC. Parameter estimation of solar cells and modules using an improved adaptive differential evolution algorithm. Appl Energ 2013;112:185–93.
[26] Gong W, Cai Z. Parameter extraction of solar cell models using repaired adaptive differential evolution. Sol Energy 2013;94:209–20.
[27] Ishaque K, Salam Z, Mekhilef S, Shamsudin A. Parameter extraction of solar photovoltaic modules using penalty-based differential evolution. Appl Energ 2012;99:297–308.
[28] Chellaswamy C, Ramesh R. Parameter extraction of solar cell models based on adaptive differential evolution algorithm. Renew Energ 2016;97:823–37.
[29] Askarzadeh A, Rezazadeh A. Artificial bee swarm optimization algorithm for parameters identification of solar cell models. Appl Energ 2013;102:943–9.
[30] Niu Q, Zhang L, Li K. A biogeography-based optimization algorithm with mutation strategies for model parameter estimation of solar and fuel cells. Energ Convers Manage 2014;86:1173–85.
[31] Askarzadeh A, Rezazadeh A. Parameter identification for solar cell models using harmony search-based algorithms. Sol Energy 2012;86:3241–9.
[32] Rajasekar N, Kumar NK, Venugopalan R. Bacterial Foraging Algorithm based solar PV parameter estimation. Sol Energy 2013;97:255–65.
[33] Awadallah MA. Variations of the bacterial foraging algorithm for the extraction of PV module parameters from nameplate data. Energ Convers Manage 2016;113:312–20.
[34] Yu K, Chen X, Wang X, Wang Z. Parameters identification of photovoltaic models using self-adaptive teaching-learning-based optimization. Energ Convers Manage 2017;145:233–46.
[35] Chen X, Yu K, Du W, Zhao W, Liu G. Parameters identification of solar cell models using generalized oppositional teaching learning based optimization. Energy 2016;99:170–80.
[36] Patel SJ, Panchal AK, Kheraj V. Extraction of solar cell parameters from a single current–voltage characteristic using teaching learning based optimization algorithm. Appl Energ 2014;119:384–93.
[37] Kler D, Sharma P, Banerjee A, Rana KPS, Kumar V. PV cell and module efficient parameters estimation using evaporation rate based water cycle algorithm. Swarm

Evol Comput 2017;35:93–110.

[38] Rezk H, Fathy A. A novel optimal parameters identification of triple-junction solar cell based on a recently meta-heuristic water cycle algorithm. Sol Energy 2017;157:778–91.

[39] Alam DF, Yousri DA, Eteiba MB. Flower Pollination Algorithm based solar PV parameter estimation. Energ Convers Manage 2015;101:410–22.

[40] Askarzadeh A, Rezazadeh A. Extraction of maximum power point in solar cells using bird mating optimizer-based parameters identification approach. Sol Energy 2013;90:123–33.

[41] Ali EE, El-Hameed MA, El-Fergany AA, El-Arini MM. Parameter extraction of photovoltaic generating units using multi-verse optimizer. Sust Energ Technol Assess 2016;17:68–76.

[42] Yuan X, He Y, Liu L. Parameter extraction of solar cell models using chaotic asexual reproduction optimization. Neural Comput Appl 2015;26:1227–39.

[43] Babu TS, Ram JP, Sangeetha K, Laudani A, Rajasekar N. Parameter extraction of two diode solar PV model using Fireworks algorithm. Sol Energy 2016;140:265–76.

[44] Guo L, Meng Z, Sun Y, Wang L. Parameter identification and sensitivity analysis of solar cell models with cat swarm optimization algorithm. Energ Convers Manage 2016;108:520–8.

[45] Wu Z, Yu D, Kang X. Parameter identification of photovoltaic cell model based on improved ant lion optimizer. Energ Convers Manage 2017;151:107–15.

[46] Allam D, Yousri DA, Eteiba MB. Parameters extraction of the three diode model for the multi-crystalline solar cell/module using Moth-Flame Optimization Algorithm. Energ Convers Manage 2016;123:535–48.

[47] Muhsen DH, Ghazali AB, Khatib T, Abed IA. A comparative study of evolutionary algorithms and adapting control parameters for estimating the parameters of a single-diode photovoltaic module's model. Renew Energ 2016;96:377–89.

[48] Ram JP, Babu TS, Dragicevic T, Rajasekar N. A new hybrid bee pollinator flower pollination algorithm for solar PV parameter estimation. Energ Convers Manage 2017;135:463–76.

[49] Muhsen DH, Ghazali AB, Khatib T, Abed IA. Extraction of photovoltaic module model's parameters using an improved hybrid differential evolution/electro-magnetism-like algorithm. Sol Energy 2015;119:286–97.

[50] Xu S, Wang Y. Parameter estimation of photovoltaic modules using a hybrid flower pollination algorithm. Energ Convers Manage 2017;144:53–68.

[51] Chen Z, Wu L, Lin P, Wu Y, Cheng S, Yan J. Parameters identification of photovoltaic models using hybrid adaptive Nelder-Mead simplex algorithm based on eagle strategy. Appl Energ 2016;182:47–57.

[52] Chen X, Xu B, Mei C, Ding Y, Li K. Teaching-learning-based artificial bee colony for solar photovoltaic parameter estimation. Appl Energ 2018;212:1578–88.

[53] Mirjalili S, Lewis A. The whale optimization algorithm. Adv Eng Softw 2016;95:51–67.

[54] Medani KBO, Sayah S, Bekrar A. Whale optimization algorithm based optimal reactive power dispatch: a case study of the Algerian power system. Elect Pow Syst Res 2018;163:696–705.

[55] Aljarah I, Faris H, Mirjalili S. Optimizing connection weights in neural networks using the whale optimization algorithm. Soft Comput 2018;22:1–15.

[56] Aziz MAE, Ewees AA, Hassanien AE. Whale optimization algorithm and moth-flame optimization for multilevel thresholding image segmentation. Expert Syst Appl 2017;83:242–56.

[57] Mafarja MM, Mirjalili S. Hybrid whale optimization algorithm with simulated annealing for feature selection. Neurocomputing 2017;260:302–12.

[58] Wang J, Du P, Niu T, Yang W. A novel hybrid system based on a new proposed algorithm-multi-objective whale optimization algorithm for wind speed forecasting. Appl Energ 2017;208:344–60.

[59] Karaboga D, Basturk B. A powerful and efficient algorithm for numerical function optimization: artificial bee colony (ABC) algorithm. J Global Optim 2007;39:459–71.

[60] Shongwe S, Hanif M. Comparative analysis of different single-diode PV modeling methods. Ieee J Photovolt 2015;5:938–46.

[61] Humada AM, Hojabri M, Mekhilef S, Hamada HM. Solar cell parameters extraction based on single and double-diode models: a review. Renew Sust Energ Rev 2016;56:494–509.

[62] Jordehi AR. Maximum power point tracking in photovoltaic (PV) systems: a review of different approaches. Renew Sust Energ Rev 2016;65:1127–38.

[63] Ishaque K, Salam Z, Taheri H. Simple, fast and accurate two-diode model for photovoltaic modules. Sol Energ Mat Sol C 2011;95:586–94.

[64] Yu K, Liang JJ, Qu BY, Chen X, Wang H, Yu K, et al. Parameters identification of photovoltaic models using an improved JAYA optimization algorithm. Energ Convers Manage 2017;150:742–53.

[65] Chen Z, Wu L, Cheng S, Lin P, Wu Y, Lin W. Intelligent fault diagnosis of photovoltaic arrays based on optimized kernel extreme learning machine and I-V characteristics. Appl Energ 2017;204:912–31.

[66] Easwarakhanthan T, Bottin J, Bouhouch I, Boutrit C. Nonlinear minimization algorithm for determining the solar cell parameters with microcomputers. Int J Solar Energy 1986;4:1–12.

[67] Prasad D, Mukherjee A, Shankar G, Mukherjee V. Application of chaotic whale optimization algorithm for transient stability constrained optimal power flow. IET Sci Meas Technol 2017;11(8):1002–13.

[68] Ling Y, Zhou Y, Luo Q. Lévy flight trajectory-based whale optimization algorithm for global optimization. IEEE Access 2017;5:6168–86.

[69] Trivedi IN, Jangir P, Kumar A, Jangir N, Totlani R. A novel hybrid PSO-WOA algorithm for global numerical functions optimization. Advances in Intelligent Systems and Computing, vol. 554. New York: Springer; 2017. p. 53–60.

[70] Alhajri MF, El-Naggar KM, Alrashidi MR, Al-Othman AK. Optimal extraction of solar cell parameters using pattern search. Renew Energ 2012;44:238–45.

[71] El-Naggar KM, Alrashidi MR, Alhajri MF, Al-Othman AK. Simulated annealing algorithm for photovoltaic parameters identification. Sol Energy 2012;86:266–74.

[72] Lin P, Cheng S, Yeh W, Chen Z, Wu L. Parameters extraction of solar cell models using a modified simplified swarm optimization algorithm. Sol Energy 2017;144:594–603.

[73] Oliva D, Aziz MAE, Hassanien AE. Parameter estimation of photovoltaic cells using an improved chaotic whale optimization algorithm. Appl Energ 2017;200:141–54.